

N 62 57585

File Copy

CASE FILE COPY

FILE COPY
NO. 1

TECHNICAL MEMORANDUMS

NATIONAL ADVISORY COMMITTEE FOR AERONAUTICS



No. 585

NATIONAL ADVISORY COMMITTEE FOR AERONAUTICS
1724 F STREET, N.W.
WASHINGTON 25, D.C.

VELOCITY DISTRIBUTION IN THE BOUNDARY LAYER

OF A SUBMERGED PLATE

By M. Hansen

From Abhandlungen aus dem Aerodynamischen Institut
an der Technischen Hochschule Aachen, No. 8, 1928

Washington
October, 1930

NATIONAL ADVISORY COMMITTEE FOR AERONAUTICS.

TECHNICAL MEMORANDUM NO. 585.

VELOCITY DISTRIBUTION IN THE BOUNDARY LAYER
OF A SUBMERGED PLATE.*

By M. Hansen.

This report deals with the measurement of the velocity distribution of the air in the vicinity of a plate placed parallel to the air flow.

I. Notation, Definitions and Theoretical Results

- ρ , density of the air,
 μ , viscosity of the air,
 ν , kinematic viscosity coefficient,
 x , distance of test point from leading edge of plate,
 y , distance of test point from plate,
 l , length of plate, 50 cm (19.69 in.),
 b , width of plate, 38 cm (14.96 in.),
 U , air velocity outside of boundary layer,
 u , component of boundary layer air velocity parallel to plate,
 δ , thickness of boundary layer,
 τ_0 , shearing stress on plate,

*"Die Geschwindigkeitsverteilung in der Grenzschicht an einer eingetauchten Platte." From Abhandlungen aus dem Aerodynamischen Institut an der Technischen Hochschule Aachen, No. 8, 1928, pp. 31-45.

$$\left. \begin{aligned} R_\delta &= \frac{U\delta}{\nu} \\ R_x &= \frac{Ux}{\nu} \\ R_y &= \frac{uy}{\nu} \end{aligned} \right\} \text{characteristic coefficients.}$$

L. Prandtl and H. Blasius succeeded in determining theoretically the velocity distribution for the case of a laminar flow.* Their results may be briefly summarized as follows.

Let x and y be the coordinates, respectively, parallel and perpendicular to the plate, and U the velocity of the undisturbed air flow. The velocity curves are similar for different values of x , the distance at which the same velocity occurs, increasing with the square root of x . The velocity obeys the law:

$$u = U f \left(y \sqrt{\frac{U}{x \nu}} \right) \quad (1)$$

For comparison with experimental results, it is convenient to introduce a "boundary-layer thickness," although no exact value can be assigned to it, because the velocity u changes asymptotically to U . For example, y may represent the boundary-layer thickness for which the function f differs from unity by a certain fraction (say 1%). If the function f in equation (1) is approximated by a parabola, which changes asymptotically into the line $u = U$, then

*H. Blasius, Zeitschrift für Mathematik und Physik, Vol. 56, No. 1, 1908.

$$y = 5.5 \sqrt{\frac{\nu x}{U}} \quad (2)$$

is then obtained for the transition point. This value of y will be taken for comparison with the experimental results.

The surface friction is represented by $\tau_0 = \mu \left(\frac{\partial u}{\partial y} \right)_{y=0}$. According to the Blasius theory, it is

$$\tau_0 = 0.332 \rho U^2 \frac{1}{\sqrt{R_x}} \quad (3)$$

Various observations led Prandtl to surmise that the laminar flow changes, with increasing Reynolds Number, to a turbulent flow, similar to the flow through a tube. Since the elementary law of turbulent friction is not yet known, the velocity distribution cannot be theoretically determined for this case. Nevertheless, if the velocity distribution experimentally determined for tubes and the likewise experimentally determined law of resistance be transferred to the case of the boundary layer, the thickness of the boundary layer can be determined with the aid of the momentum theorem even for this case. This calculation was made by Prandtl and Von Karman.* The thickness of the boundary layer was found to be

$$\delta = 0.370 R_x^{-1/5} \quad (4)$$

The shearing stress was

$$\tau_0 = 0.0225 \rho U^2 \left(\frac{U \delta}{\nu} \right)^{-1/4} \quad (5)$$

*Zeitschrift für angewandte Mathematik und Mechanik, Vol. I, 1921, pp. 233-298.

The fundamental velocity distribution for

$$0 < y < \delta \quad \text{is} \quad u = U \left(\frac{y}{\delta} \right)^{1/7} \quad \text{and for } y > \delta \quad \text{is} \quad u = U.$$

II. Researches of Burgers and Zijnen

In 1923-1925, J. M. Burgers and B. G. van der Hegge Zijnen, in the Aerodynamical Institute of the Delft Technical High School, investigated the velocity distribution in the boundary layer for both kinds of flow and particularly in the region of transition from the laminar to the turbulent state.* In the laminar region they found very good agreement between the theoretical and experimental results, as regards the thickness of the boundary layer. The discrepancies were greater, however, as regards the shearing stresses, whether determined from the velocity gradient on the plate, or from the momentum theorem with the help of the formula

$$\tau_0 = \frac{d}{dx} \rho \int_0^{\delta} u (U - u) dy \quad (6)$$

The point of transition from the laminar to the turbulent region could be quite accurately determined by plotting the measured boundary-layer thickness as a function of the coordinate x .

The resulting curve has a sharp bend at a certain value of R_x . This value of R_x may be designated as the "critical characteristic" (Kennzahl). On the other hand, a "characteristic" can

be assigned to the boundary layer itself, by expressing it in

*"Measurements of the Velocity Distribution in the Boundary Layer Along a Plane Surface," Delft, 1924.

the form $R_\delta = U\delta/\nu$. R_δ and R_x are theoretically connected by the expression $R_\delta = 5.5 \sqrt{R_x}$, which was also approximately confirmed by experiment. The measurements showed that R_δ varies between 1650 and 3500 and is therefore considerably greater than in tubes. In the turbulent region the measurements showed that the velocity varied approximately as $\sqrt[3]{y}$. The curve of the boundary-layer thickness does not correspond to the formula $\delta = 0.37 x R_x^{-1/5}$, because in its derivation, it was assumed that the turbulent flow begins at $x = 0$, though, in reality, the laminar flow continues up to the critical value of R_x . Zijnen extended the formula by introducing a parameter x_0 and putting

$$\delta = 0.37 (x - x_0)^{4/5} \left(\frac{\nu}{U}\right)^{-1/5} \quad (7)$$

in which x_0 depends particularly on the shape of the leading edge of the plate (sharp or rounded). The experimental results can be represented very well by this modified formula.

III. Object of Recent Experiments - Laboratory Equipment

My own experiments were intended, on the one hand, to account for the discrepancies in the above-mentioned experiments and, on the other hand, to determine the velocity distribution on rough plates. The means for these experiments were placed at my disposal by the "Notgemeinschaft der Deutschen Wissenschaft" (Emergency Fund for the Promotion of German Science).

The experiments were performed in the small wind tunnel

belonging to the Aerodynamic Institute of the Aachen Technical High School (Figs. 1-2). The diameter of the entrance cone is 30 cm (11.8 in.). The length of the free jet between the entrance and exit cones is about 2.5 m (8.2 ft.). The measurements were made in this free jet where the static pressure was constant, which was essential for the method of measurement used.

The wind velocity U was accurately controlled by enlarging or diminishing the exit opening a by the use of plates. It was not feasible to regulate the wind velocity by means of a slide valve at a point b of the enclosed portion of the wind tunnel, because this disturbed the air flow too much. This method was used, however, to produce artificial turbulence. Figure 3 shows the plates used in the tests, together with their degrees of roughness. The plates were successively mounted in a wooden frame on the test stand. Underneath the plate and mounted on a block of concrete, there was a lathe bed which supported the measuring instrument. This arrangement made it possible to move the measuring instrument either parallel or perpendicular to the plate. x was read on a scale parallel to the plate. The perpendicular distance y from the surface of the plate was measured to within 0.01 mm (.0004 in.) by a slide gauge mounted on the same support. The pressure was determined by means of two alcohol pressure gauges. The temperature and pressure were read frequently during the tests.

Though the Delft measurements were made with a hot-wire

instrument, I decided to use small Pitot tubes, which are comparatively easy to make by drawing out and bending the ends of very small glass tubes. The smallest tube drawn by me had an outside diameter of 0.135 mm (0.0053 in.). They worked so slowly, however, that the readings would have taken too much time.

Tube No. 13, with an outside diameter of 0.35 mm (0.0138 in.) and an inside diameter of 0.31 mm (0.0083 in.), was the most satisfactory and was used for most of the measurements. Figure 4 shows the calibration curves of this tube. The results obtained with it were then compared with those obtained with an ordinary Pitot tube. If discrepancies were found, they could be mostly eliminated by grinding the open end of the tube. The measurements could be made only in a velocity region of 4 to 36 m/s (13 to 118 ft./sec.), since the tubes vibrated strongly at higher speeds.

In order to determine the distance between a tube and the plate, I had to find the position at which the tube touched the plate. This position was easily determined by observing when the tip of the tube and its image came together (Fig. 5).

A sufficiently accurate adjustment of the plate was effected by mounting it perpendicular to the plane of the Pitot tube with the aid of a carpenter's square. Any more accurate adjustment did not appear necessary, since measurements on both sides of the plate showed that the results were hardly affected by a slight obliqueness of the plate.

IV. Results

a) Laminar Flow

Figure 6 shows the results for the thin dural plate No. 1. It is seen that the measured velocity distribution agrees very well with the theoretically calculated velocity. The velocity ratio is plotted as a function of the quantity $y/\sqrt{\frac{\nu x}{U}}$, and shows that, within the accuracy of the measurements, the sections very well obey the law of similarity.

In Figure 7 the thickness of the boundary layer is plotted as a function of the quantity $\sqrt{\frac{\nu x}{U}}$ and likewise agrees well with the theory.

For the thicker plate No. 4 (Figs. 8-9), the first sections, with small values of x , show systematic deviations which disappear for thicker sections.

Figure 10 gives a verification of the impulse balance by comparing the shearing stress, as determined from the velocity gradient, with the value obtained from the momentum by means of formula (6). As shown in the figure, the two values obtained from my experiments agree very well, while there is a discrepancy in the values obtained from the measurements by Burgers. In my experiments there are differences at the leading edge of the plate. Hence it may be inferred that the slight discrepancies in my measurements are due to the influence of the leading edge, while there must be some other reason for the discrepan-

cies in the measurements made by Burgers.

In order to ascertain the effect of the finite thickness of the plate, especially the difference between the rounded and sharpened plates, I tried first to calculate the potential flow and then the curve of the boundary-layer thickness for such plates. The potential flow was calculated by the so-called inverse method, by assuming source distributions which, when superposed on the parallel flow, yielded streamline shapes similar to the plates used by me. The rounded section can be generated by pointlike sources, while distributed sources must always be adopted if the sharp section is to be substituted.

Figure 11 shows the velocity curve calculated from the source distribution. In addition to the velocity curve, its first and second differential quotients are given according to the length of the arc, because these quantities are necessary to determine the thickness of the boundary layer. This thickness was calculated by A. Pohlhausen's method (Abh. Aerodyn. Inst. Aachen, No. 1). Figure 12 shows the course of the quantity $z = \delta^2/\nu$ for both the cases represented in Figure 11. With the rounded plate (pointlike source) the thickness of the boundary layer increases very rapidly and separation soon occurs. With the sharp-edged plate (linear source distribution), on the other hand, the deviation from the Blasius case (infinitely thin plate) is not very great. This result is in accord with the observed fact that, even at a short distance from the leading edge of the

rounded plate, the boundary layer becomes turbulent, while with the sharp-edged plate the laminar flow persists much longer.

As regards the experiments of Burgers and Zijnen, this calculation could not explain the great discrepancy between the theoretical and experimental results as found, e.g., in the velocity gradient on the wall of the tunnel. The calculation might be utilized at most to explain the S-shaped velocity curve found by the above-mentioned investigators. The boundary-layer theory, in fact, gives such curves, provided a pressure increase or velocity decrease ($U' = \frac{d u}{d x} < 0$ in Fig. 11) is present.

The reason why Burgers and Zijnen found a considerable deviation from the theory of Blasius, while my measurements show a much better agreement, is due, in my opinion, to the fact that the Delft experiments were performed in a closed wind tunnel, while mine were made in a free air stream. In a closed wind tunnel, a decrease in pressure or an increase in velocity, corresponding to the frictional resistance of the tunnel walls and of the plate itself, must take place outside the boundary layer. The air flowing between the tunnel wall and the test plate is in a similar state to that in the first part of a tube. The resulting deviations from the Blasius theory can be approximately calculated, since Zijnen himself established the increase in velocity along the test plate, though for another purpose (Thesis, Report No. 6, Delft, 1924, pp. 39-42). He expressed the

mean velocity increment by $\frac{dU}{dx} = \frac{\beta}{l} U$. The factor β denotes the velocity increment for the entire length l as a fraction of the velocity U . For example, Zijnen found that $\beta =$ about 0.06 for $U = 8$ m/s (26 ft./sec.). I have investigated the effect of the velocity increment on the thickness of the boundary layer according to K. Pohlhausen's method and found smaller values for the thickness than the Blasius theory would lead one to expect. In fact, the Delft measurements show a deviation of the same nature. The velocity gradients on the plate can be compared for the two cases. For this purpose, in the calculation of the boundary-layer thickness, I introduced Zijnen's experimentally found values for δ and the above value for $U' = \frac{dU}{dx}$ into Pohlhausen's differential equation for the boundary layer. The result is shown in Figure 13. The plain lines represent the velocity gradient according to the Blasius method, while the dash lines represent the same according to my own method, with allowance for the velocity gradient in the tunnel. The agreement is very good up to the last value, which corresponds to a velocity curve at the distance $x = 62.5$ cm (24.6 in.) from the leading edge of the plate. With this velocity curve the transition to the turbulent condition has evidently taken place already, so that agreement can no longer be expected.

The above-mentioned calculation also shows that the boundary-layer formation is very sensitive to relatively slight local variations in the velocity of the air flow along the plate so

that such measurements must really be linked with a very accurate control of the static pressure. Thus, even an undulating or wavy shape of the plate may affect the formation of the laminar boundary layer.

b) Transition from Laminar to Turbulent Flow

We have already remarked that the boundary layer can be assigned a critical characteristic value $R_\delta = 5.5 \sqrt{R_x}$, at which the transition from the laminar to the turbulent condition takes place. I have attempted to determine R_δ by two methods. The transition is evidenced, on the one hand, by a sudden growth of the boundary layer and, on the other hand, by the development of a shearing stress. Zijnen determined R_δ by plotting the boundary-layer thickness. In a similar manner (Fig. 14) I first plotted the nondimensional quantity $\delta / \sqrt{\frac{\nu x}{U}}$ and then also the quantity $\frac{\tau}{U^{3/2} (\nu x)^{-1/2}}$ as a function of the characteristic value. Both quantities must be constant for a purely laminar boundary layer.

Despite the scattering of the test points, a bend is quite clearly indicated at $R_\delta =$ about 3100. This result agrees with the Delft measurements. If this value of R_δ is compared with the critical characteristic of tubes or rings, it appears very high. If it is considered, for example, that the thickness of the boundary layer should logically be taken as the hydraulic radius in our case, R_δ would have a value about six times as

large as the corresponding value for tubes. It should be noted, however, that, even for tubes and rings, the value of the critical characteristic can be greatly increased by a steady inflow. In the case of the sharp-edged plate, we have only a comparatively steady flow. If the flow is disturbed, e.g., by the separation of the boundary layer on a rounded leading edge, the transition takes place at a lower characteristic value. Also when the air stream itself, for example, due to strong throttling, was more turbulent than under normal conditions, I found that the reversal occurred sooner. The lower limit of R_δ has not yet been established. Figures 15-16 give examples of velocity distribution in the transition region.

c-1) Turbulent Flow over a Smooth Plate

Since the preliminary experiments showed that the transition to the turbulent flow is accelerated by rounding the leading edge of the plate, a rounded strip of wood was applied to the front edge of the glass plate. With this arrangement a turbulent flow had already developed at $x = 10$ cm (3.94 in.). The tests covered a velocity range of 16 to 36 m/s (52-118 ft./sec.). Between $x = 10$ cm (3.94 in.) and 50 cm (19.69 in.), measurements were made on the plate section at intervals of 5 cm (1.97 in.). The corresponding shearing stresses on the wall were determined from formula (6). No direct determination of the shearing stresses on the wall could be made with the help of the ve-

locity gradient, because the measurement with the Pitot tube did not give sufficiently accurate results close to the wall. The results of the measurements are shown in Figure 17, both the distance from the wall and the velocity being plotted logarithmically. It is obvious that, disregarding the immediate proximity of the wall ($y < 1$ mm), the velocity distribution can be quite well approximated by a potential law.

In Figure 18, the velocity ratio u/U is likewise logarithmically represented as a function of the ratio y/δ . The values of δ were derived from the points of intersection of the sloping lines in Figure 17 with the horizontal lines in u/U . In other words, the lines corresponding to the different values of x were brought into coincidence by shifting horizontally. Figure 18 shows that the slope of the lines, i.e., the exponent of the potential expression depends somewhat on the velocity.

If we put

$$\frac{u}{U} = c \left(\frac{y}{\delta} \right)^n \quad (c = \text{proportionality factor}) \quad (8)$$

the exponent n then increases with the velocity. For example:

$$n = 0.186 \quad \text{for } U = 20 \text{ m (65.6 ft.)};$$

$$n = 0.196 \quad \text{" } U = 28 \text{ " (91.9 ")};$$

$$n = 0.198 \quad \text{" } U = 36 \text{ " (118.0 ")}.$$

The exponents obtained for the smooth plate by this method are all higher than the exponent $n = 1/7 = 0.143$ derived by Prandtl and von Karman from the law of resistance. This is due in part to the fact that the test points $y < 1$ mm were disregarded in

in the evaluation.

If the velocity distribution is approximated by a potential law, the integral in formula (6) can then be evaluated. If the boundary-layer thickness is introduced in the above-mentioned sense, it is found that

$$\tau_0 = \frac{d}{dx} \frac{\delta}{x} a \rho U^2 \quad (9)$$

in which the quantity a is connected with the exponent n by the expression

$$a = \frac{1}{n+1} - \frac{1}{2n+1}$$

I have usually determined the shearing stress with the aid of formula (9).

If it is assumed that, between the shearing stress, the distance from the tunnel wall and the velocity, there exists a definite relation governed only by the physical constants, density and viscosity, this relation can then be expressed in the form

$$\frac{\tau_0}{\rho u^2} = f \left(\frac{u y}{\nu} \right) \quad (10)$$

This equation is the usual mathematical expression of the Prandtl dimensional consideration, which leads to the previously mentioned formula for the turbulent velocity distribution. The quantity uy/ν can be regarded as a kind of characteristic coefficient R_y for the point y . If the velocity distribution is approximated by a potential formula, equation (10) is changed to

$$\frac{\tau_o}{\rho u^2} = \zeta \left(\frac{u y}{\nu} \right)^m \quad (11)$$

The relation between the exponents n and m is evidently expressed by the formula $m = -\frac{2n}{n+1}$. ζ is a coefficient which can be determined from the measurements.

Theodor von Karman, on the basis of the Blasius law of resistance, arrived at the values: $\zeta = 0.0225$, $m = 0.25$, $n = 0.143$. I have compared all the data obtained for the smooth plate with the von Karman theory (Fig. 19). It is seen that the points for small values of uy/ν , in the vicinity of $uy/\nu \leq 2000$, scatter about the theoretical curve, which a systematic deviation occurs for greater values. Greater values than $n = 0.143$ are likewise obtained by disregarding the values in the immediate vicinity of the tunnel wall, as already mentioned.

c-2) Turbulent Flow along Rough Plates

After the measurements on the smooth plate, I determined the velocity distribution on an undulating plate and on two rough plates. It was found that the interpolation with the potential formula gave good results even in this case. The data were worked out in the same manner as for the smooth plate (Figs. 20-22).

Furthermore, the resistance and the shearing stress were determined from the impulse integral. For comparison I determined the integral first on the basis of the test points, but

then also with the aid of formula (9). The deviations were greater for the rougher plate, apparently because the interpolation with the aid of the potential law does not hold good up to values of $u = U$ or $y = \delta$, but the velocity-distribution curve is sharper. In this case the exact integral was naturally resorted to for the calculation of the shearing stress.

The next step was to determine to what extent the shearing stress can be represented by formula (11). Figures 23 and 24 show the result. The quantity $\tau_0/\rho u^2$ is plotted as the ordinate and uy/v as the abscissa, both in the logarithmic scale. It is obvious that the absolute value of the exponent m increases, on the one hand, with increasing roughness and, on the other hand, with increasing velocity.

For all the data, the coefficient ζ varies between 0.03 and 0.6, the exponent m between -0.3 and -0.5 and correspondingly the exponent n between 0.186 and 0.325. I have now made the noteworthy observation that the values of ζ , as a function of n in the logarithmic scale, lie on a straight line.

In my opinion, the fundamental importance of the results resides in the fact that there is apparently a definite relation between the exponent of the velocity distribution and the coefficient ζ . The latter corresponds to the coefficient which is assumed to be constant in the theory for the ideal case of the smooth plate. For rough plates, however, both the quantity ζ and the exponent m are no longer constants, but are affected

by the velocity as well as by the roughness. It may be surmised that both depend on the nondimensional quantity $u\kappa/\nu$, in which κ is the mean roughness. The general resistance formula would then have the form

$$\frac{\tau_0}{\rho u^2} = \left(\frac{u \nu}{\nu}\right)^{m\left(\frac{u \kappa}{\nu}\right)} \zeta\left(\frac{u \kappa}{\nu}\right) \quad (12)$$

It is still uncertain whether this equation represents only an interpolation formula or a definite law.

Translation by
National Advisory Committee
for Aeronautics.

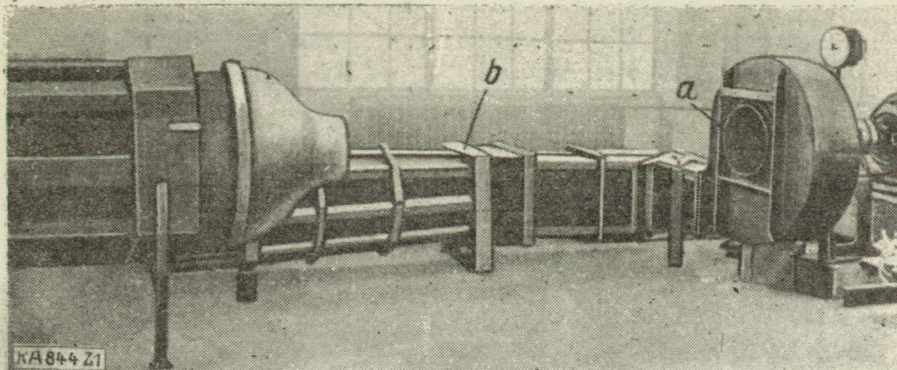


Fig. 1

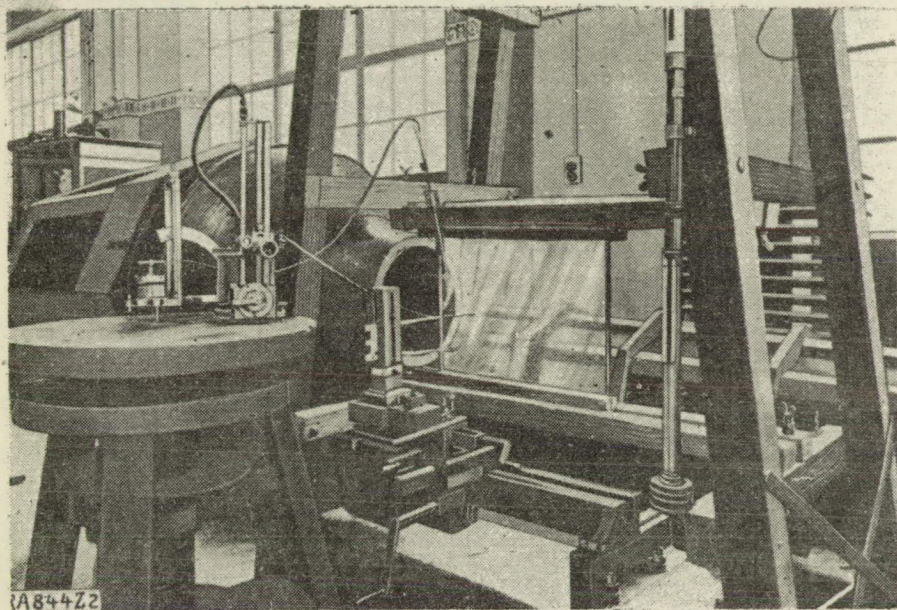


Fig. 2

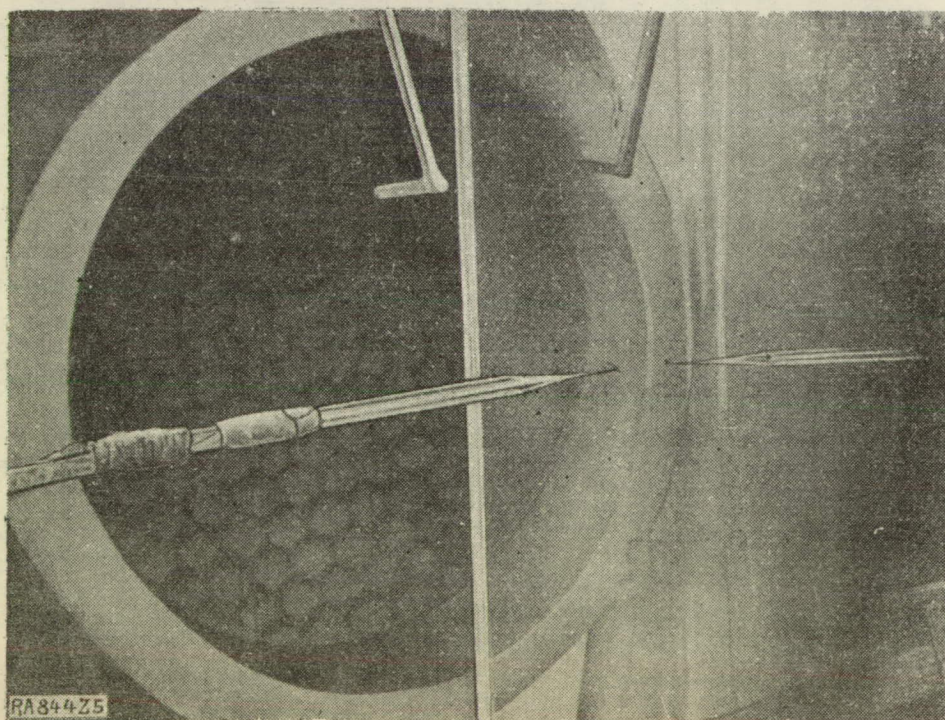
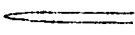
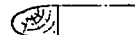
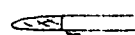
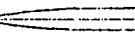
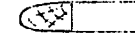
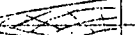


Fig. 5

No.	Plate	Thick-ness	Leading edge
1	Sheet dural (smooth)	2.5 mm	 Sharp
2	Glass (smooth)	9.0 mm	 Rounded
3	" "	4.5 mm	 Sharp Turbulence
4	Sheet dural (smooth)	6.0 mm	 Sharp
5	Glass (undulating)	8.0 mm	 Rounded
6	Glass (roughness I)	15.0 mm	 Sharp
7	Glass (roughness II)	3.5 mm	 Rounded

Length of plates, $l = 50$ cm

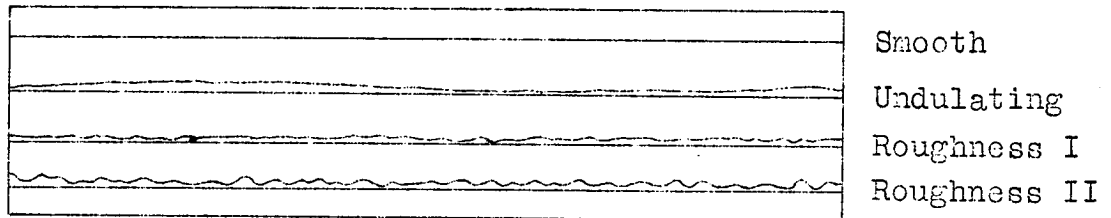
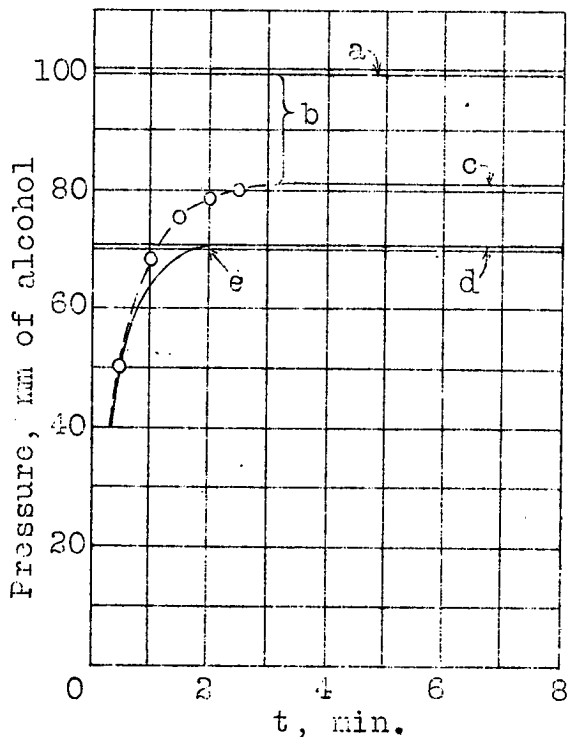
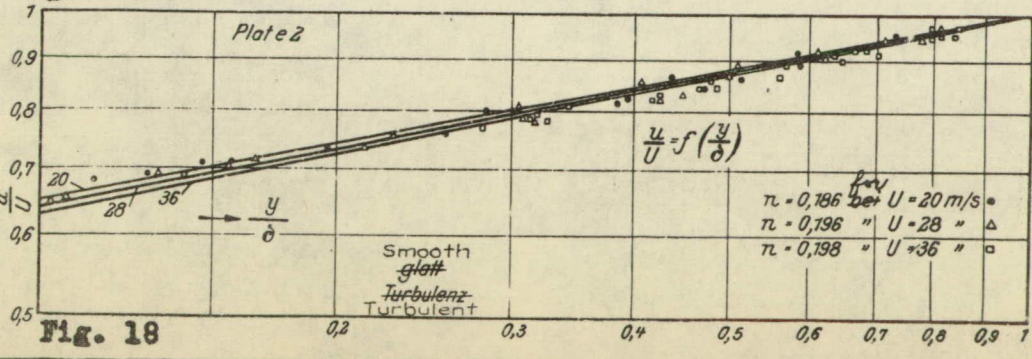
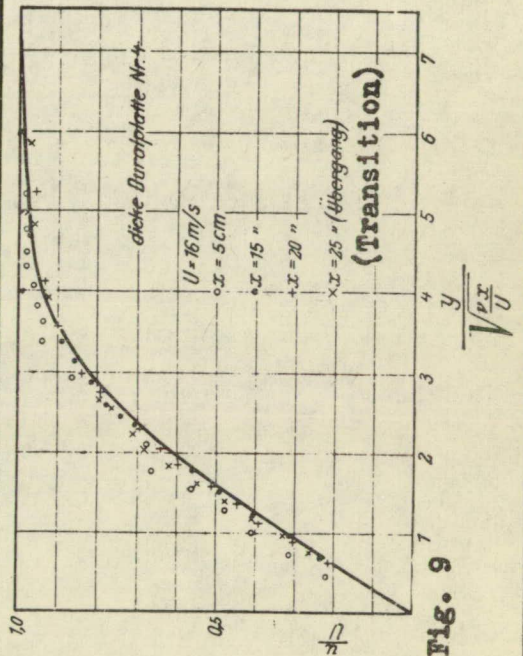
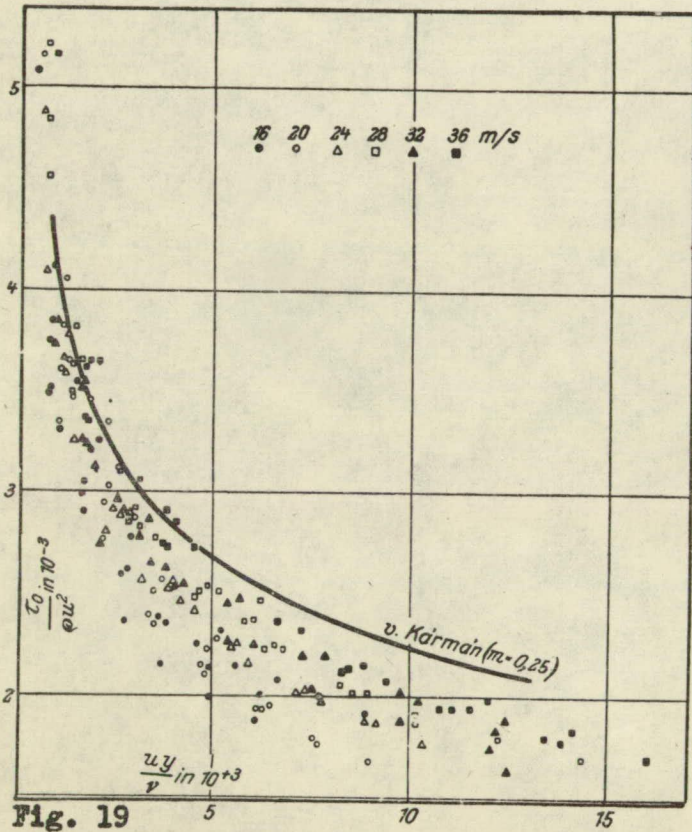
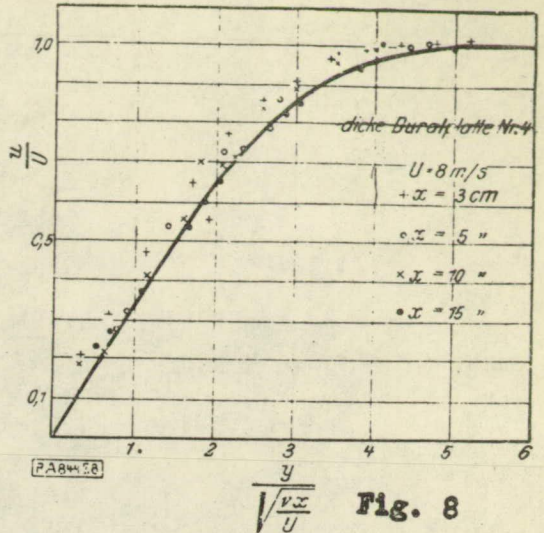
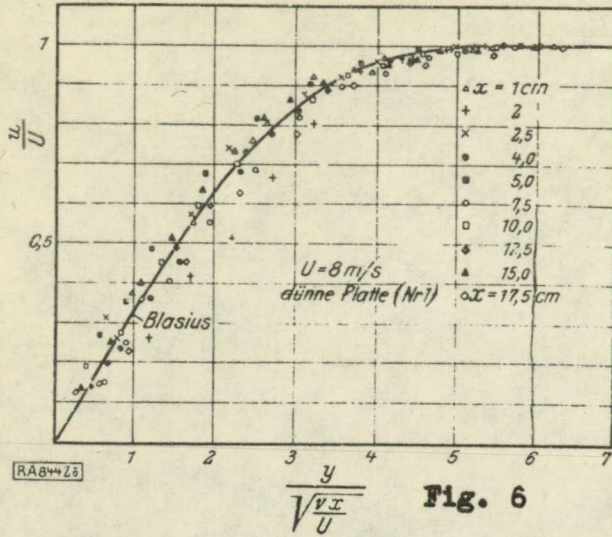


Fig. 3



- a, Result with large pitot tube.
- b, Difference in results.
- c, Result with tube No. 13 before grinding and after grinding the open end.
- d, The result with large and small tubes agree.
- e, No difference

Fig. 4 Calibration curves of tube No. 13



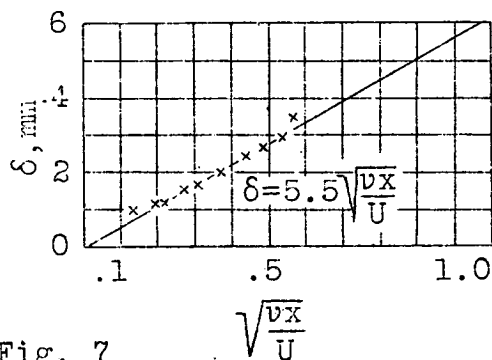


Fig. 7

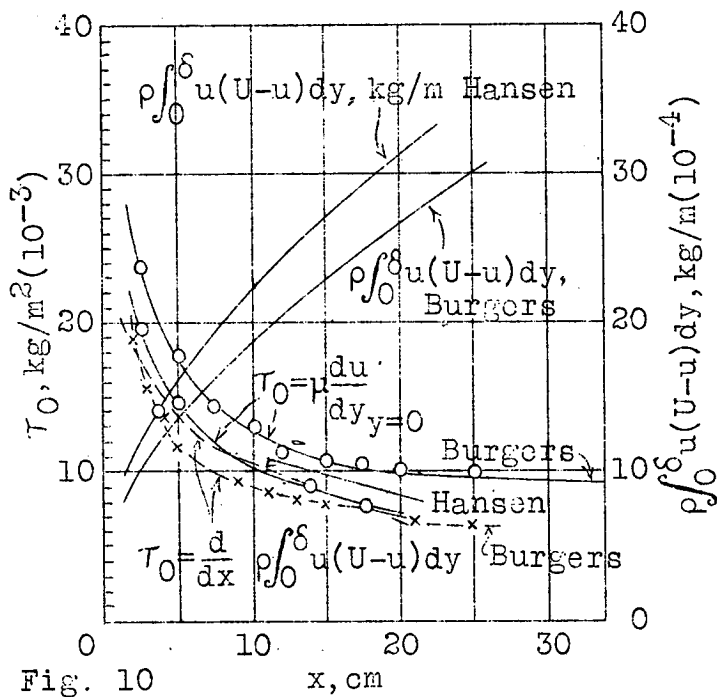
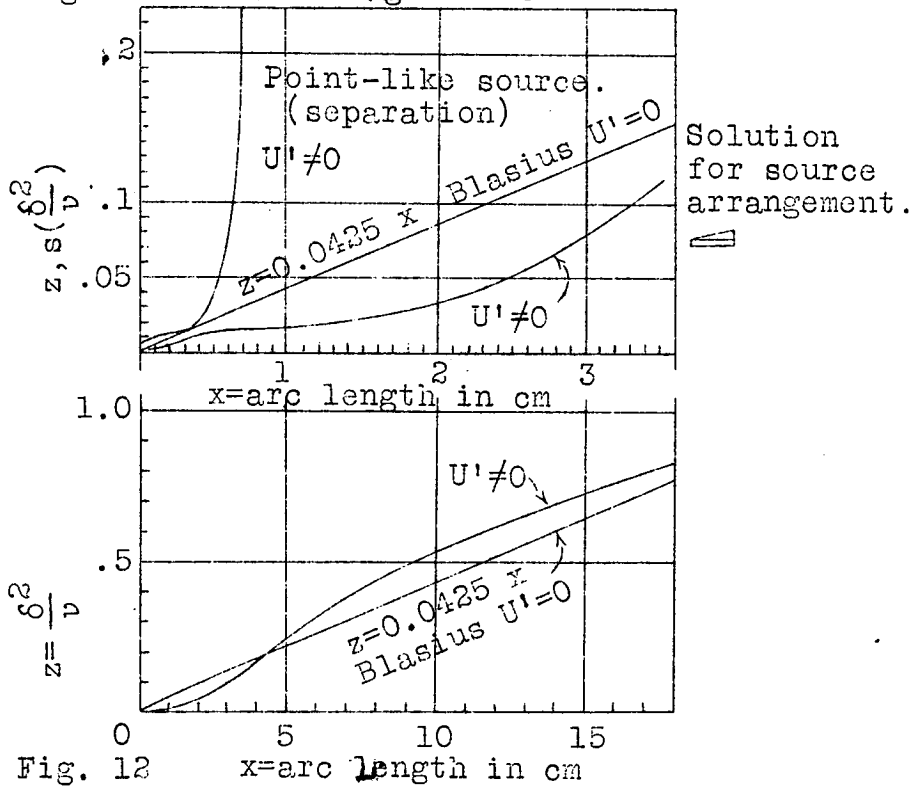
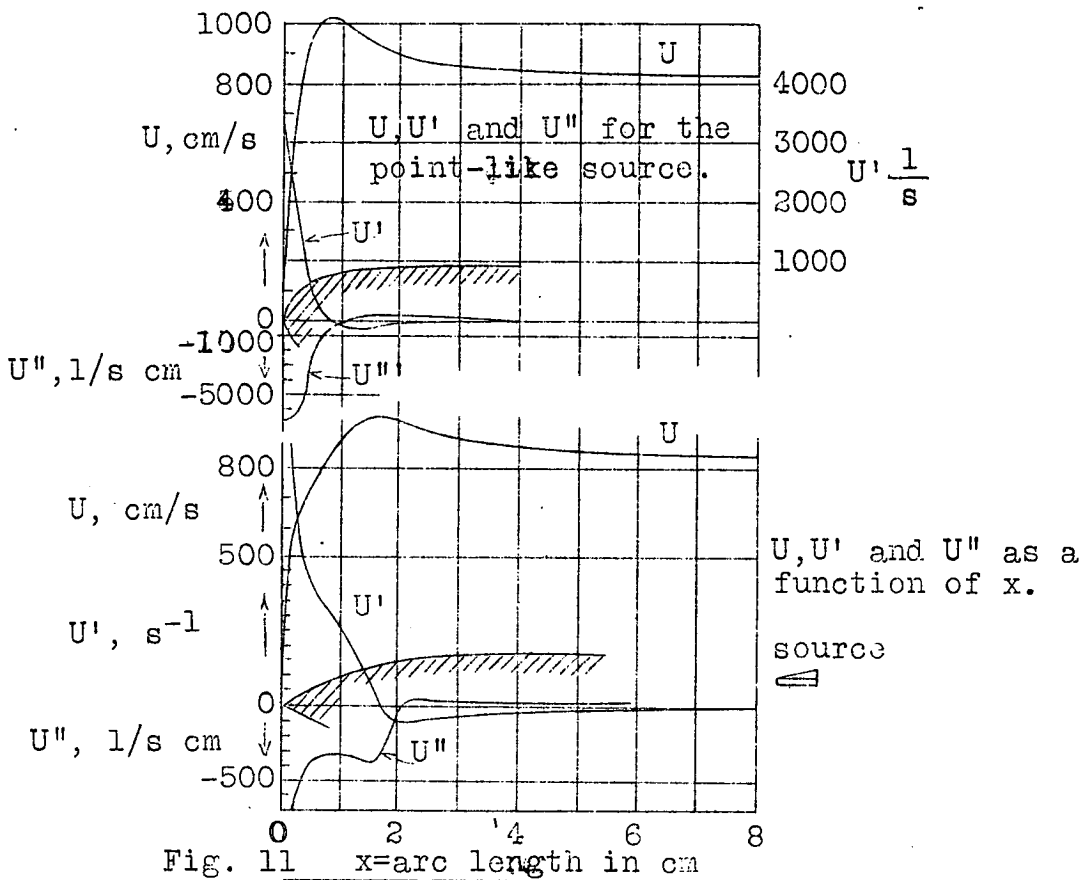


Fig. 10



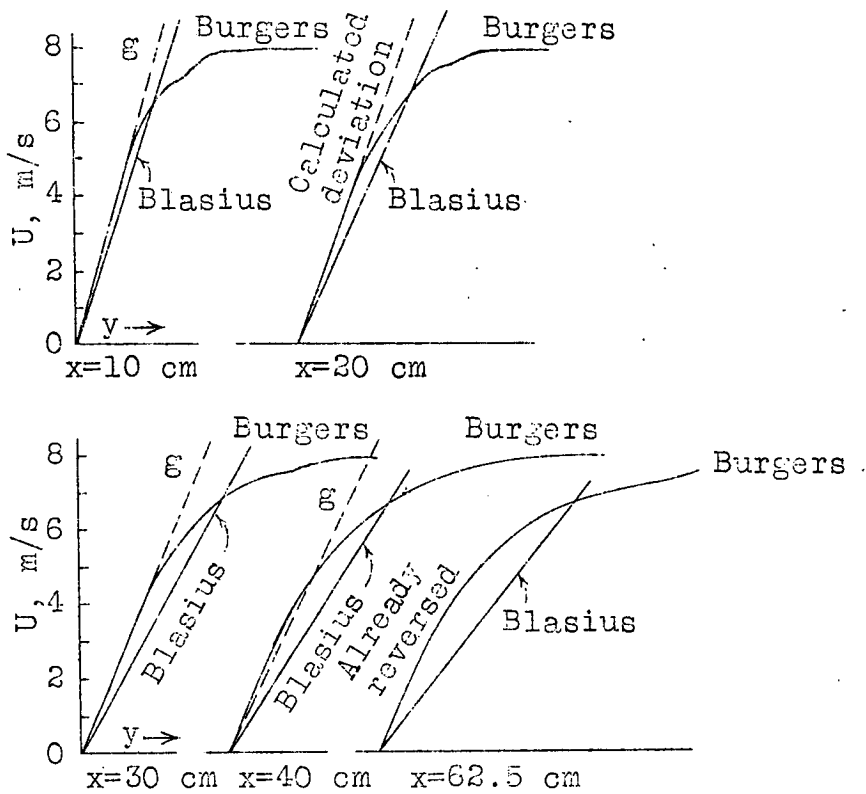


Fig. 13

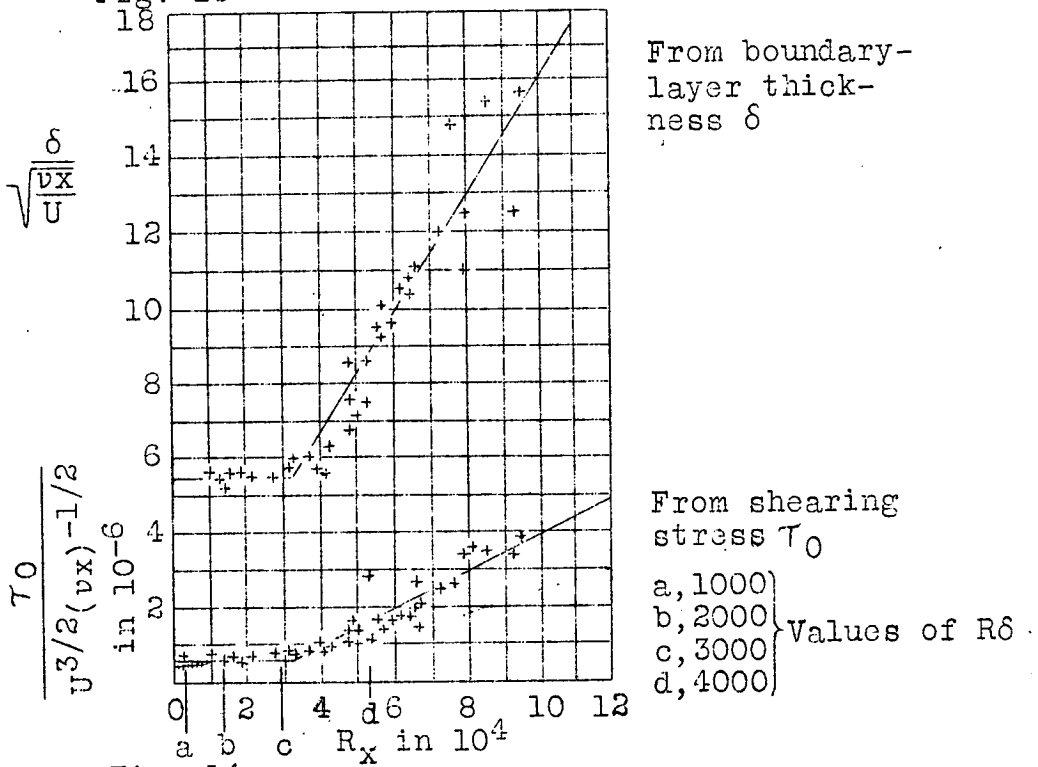


Fig. 14

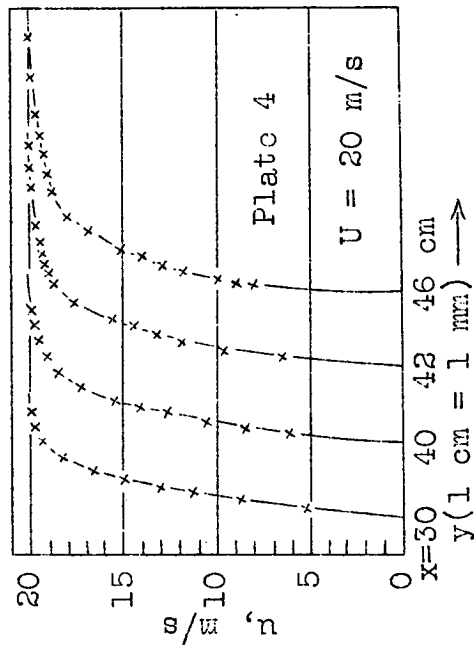
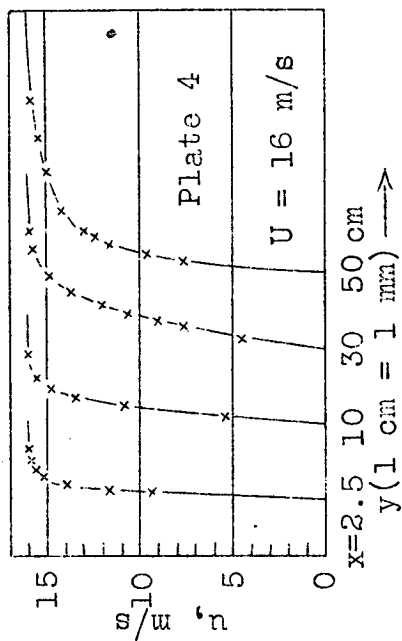


Fig. 15

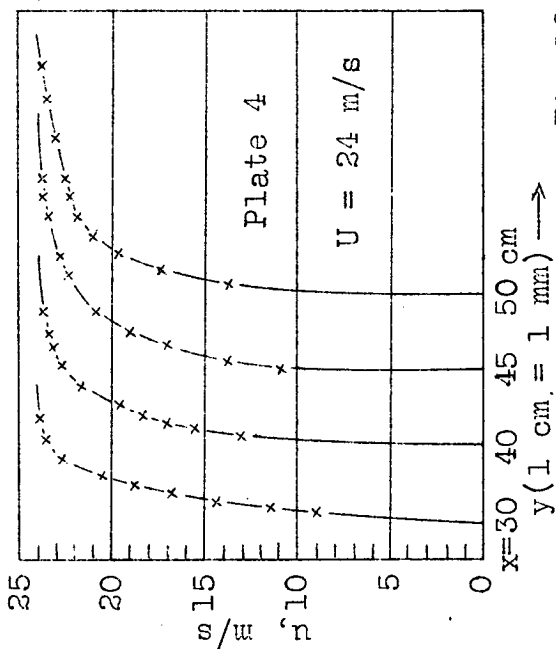
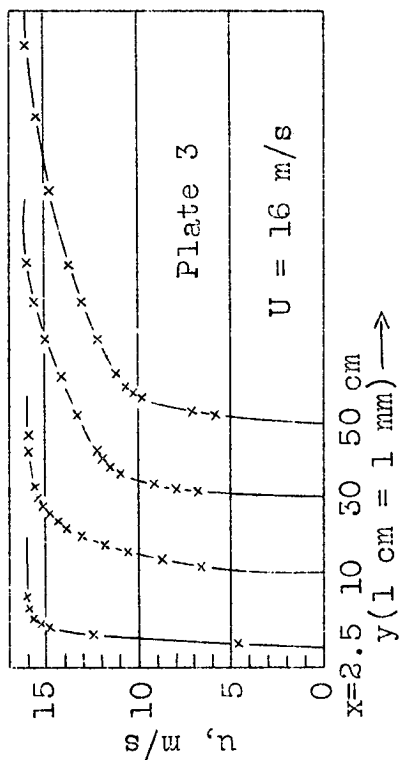


Fig. 16

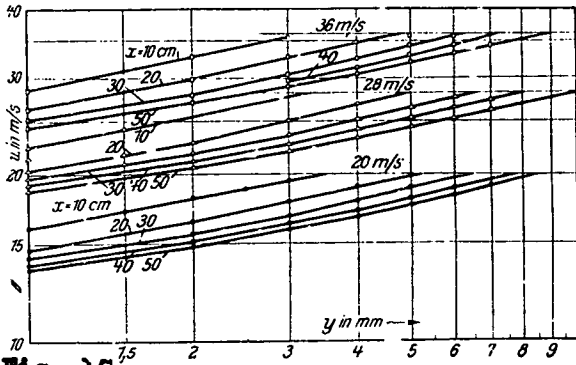


Fig. 17

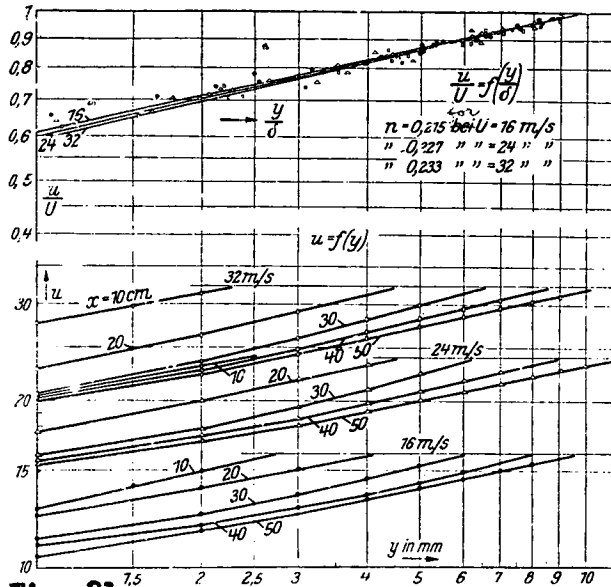


Fig. 21

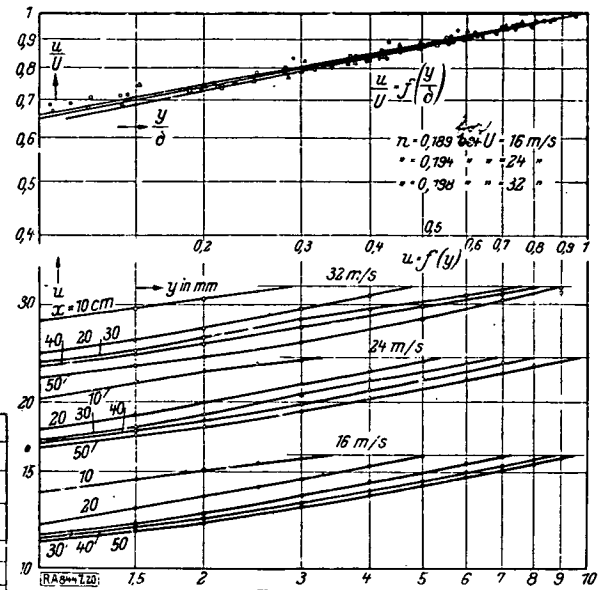


Fig. 20

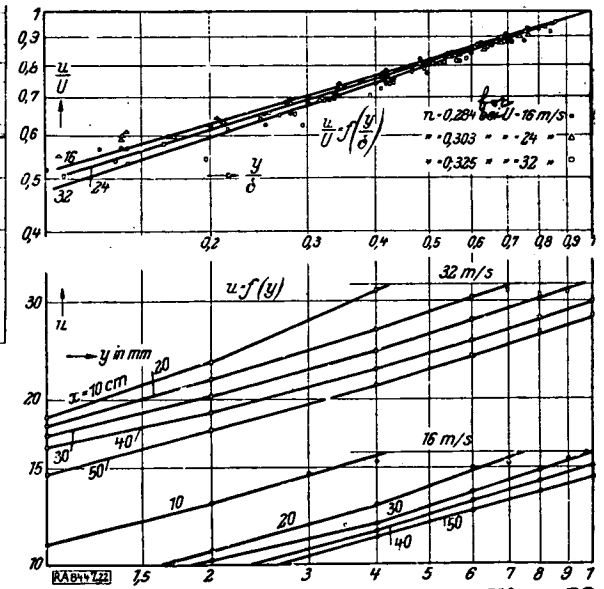


Fig. 22

- a = smooth
- b = wavy
- c = roughness I
- d = roughness II

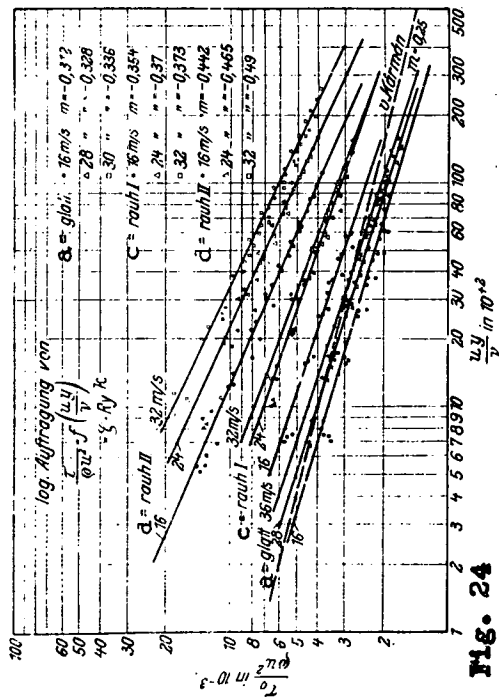


Fig. 24

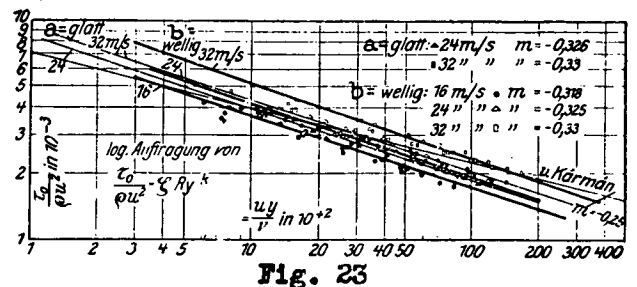


Fig. 23